Effect of calcium phosphate heparinization on the *in vitro* inflammatory response and osteoclastogenesis of human blood precursor cells

A.Diez-Escudero,[1,2] E. Torreggiani[3], G. Di Pompo[3], M. Espanol[1,2], C. Persson[4], G. Ciapetti[3], N. Baldini[3,5] and M.-P. Ginebra[1,2,6] *

[1] *Biomaterials, Biomechanics and Tissue Engineering Group, Dept. Materials Science and Metallurgical Engineering. Universitat Politècnica de Catalunya (UPC), Av. Eduard Maristany 16, 08019 Barcelona, Spain.*
[2] *Barcelona Research Center in Multiscale Science and Engineering, UPC, Eduard Maristany 16, 08019 Barcelona, Spain.*
[3] *Orthopaedic Pathophysiology and Regenerative Medicine Unit, IRCCS Istituto Ortopedico Rizzoli, Bologna, Italy*
[4] *Applied Material Science, Department of Engineering Sciences, The Ångstrom Laboratory, Uppsala University, SE-751 21, Uppsala, Sweden*
[5] *Department of Biomedical and Neuromotor Sciences, University of Bologna, Bologna, Italy.*
[6] *Institute for Bioengineering of Catalonia, Barcelona Institute of Science and Technology, Baldiri Reixac 10-12, 08028 Barcelona, Spain.*

anna.diez@angstrom.uu.se,   *trrlne@unife.it,*   *gemma.dipompo@ior.it,*

montserrat.espanol@upc.edu,   *cecilia.persson@angstrom.uu.se,*   *gabriela.ciapetti@ior.it,*

nicola.baldini@ior.it, maria.pau.ginebra@upc.edu

*Corresponding author

Abstract

The immobilization of natural molecules on synthetic bone grafts stands as a strategy to enhance their biological interactions. During the early stages of healing, immune cells and osteoclasts (OC) modulate the inflammatory response and resorb the biomaterial, respectively. In this study, heparin, a naturally occurring molecule in the bone extracellular matrix, was covalently immobilized on biomimetic calcium-deficient hydroxyapatite (CDHA). The effect of heparin-functionalized CDHA on inflammation and osteoclastogenesis was investigated using primary human cells, and compared to pristine CDHA and beta-tricalcium phosphate (β-TCP). Biomimetic substrates led to lower oxidative stresses by neutrophils and monocytes than sintered β-TCP, even though no further reduction was induced by the presence of heparin. In contrast, heparinized CDHA fostered osteoclastogenesis. Optical images of stained TRAP positive cells showed an earlier and higher presence of multinucleated cells, compatible with OC at 14 days, whilst pristine CDHA and β-TCP present OC at 21-28 days. Although no statistically significant differences were found in the OC activity, microscopy images evidenced early stages of degradation on heparinized CDHA, compatible with osteoclastic resorption. Overall, the results suggest that the functionalization with heparin fostered the formation and activity of OC, thus offering a promising strategy to integrate biomaterials in the bone remodeling cycle by increasing their OC-mediated resorption.

Keywords: Biomaterial, heparin, hydroxyapatite, inflammation, osteoclastogenesis

1. Introduction

The success of synthetic bone grafts upon implantation is usually related to their ability to favorably modulate the host response. The interactions of the biomaterial with the host tissue mainly involve the immune and the skeletal systems in what nowadays is known as osteoimmunology (Franz, Rammelt, Scharnweber, & Simon, 2011). The immune system plays a role in the inflammatory response upon implantation, while the skeletal system will orchestrate the osteogenic/osteoclastogenic response of bone to interact with the biomaterial (Anderson, Rodriguez, & Chang, 2008). The resolution of this first inflammatory response is a required key-step for the consequent tissue repair and regeneration. The main actors involved in inflammation are the blood cells arriving to the injured site by extravasation. Neutrophils, monocytes and monocyte-derived cells, such as macrophages, are the first interacting cells. These trigger the biological cascade by releasing reactive oxygen and nitrogen species (ROS and RNS respectively), chemokines and cytokines (Zhang et al., 2013). Hence, the modulation of this early response has recently drawn the attention of the scientific community in an effort to enhance the tissue regeneration potential of biomaterials.

Reducing or controlling inflammation upon implantation is a strategy that can foster the success of an implanted material (Loi et al., 2016). One interesting approach is the use of glycosaminoglycans (GAGs) as anti-inflammatory molecules. Hyaluronic acid, chondroitin sulphate and heparin have shown good anti-inflammatory properties by binding to chemo- and cytokines (Severin et al., 2012). The relevance of GAGs as inflammation mediators *in vivo* has recently been shown by their interaction with pro-inflammatory chemokines, such as interleukin–8 (CXCL8)/neutrophil-mediated inflammation (Gschwandtner et al., 2017). In addition, GAGs are part of the extracellular matrix (ECM), and they are known to interact with several signaling proteins involved not only in the immune system but also in the skeletal regulatory pathways (Capila & Linhardt, 2002). Recent studies have highlighted the affinity of

GAGs for osteogenic proteins such as bone morphogenetic proteins (BMPs) (Bramono et al., 2012), thanks to the presence of heparin binding domains in BMPs. The degree of sulfonation of GAGs has been pointed as a key to control such interactions (Hempel et al., 2014). Human BMP-4 showed higher binding affinity to oversulfated GAGs compared to those lacking sulfate groups (Hintze et al., 2009). Whereas the osteogenic potential of GAGs, and specifically heparin has been reported, the effect on osteoclastogenesis has not yet been explored in combination with biomaterials, although studies have reported the singular effect as a supplement in cell culture media. Supplementation of sulfonated GAGs combined with collagen matrices or in cell culture media has shown to promote osteoblast (OB) activity and osteoclast adhesion and viability (Salbach-Hirsch, 2014; Salbach et al., 2012) but suppress OC activity when using OB supernatants previously in contact with GAGs. On the other hand, the direct supplementation of heparin in cell culture media using RAW murine cells also showed that osteoclast formation was promoted following dual exposure to RANKL and OPG: heparin-bound OPG was found to increase the amount of RANKL available for OC maturation (Irie et al., 2007; Ling, Murali, Stein, van Wijnen, & Cool, 2010).

Contrary to the aforementioned studies in which authors have solely investigated the effect of GAGs on osteogenic lineage by supplementing different GAGs to cell culture medium, in this study, we propose to exploit the capacity of GAGs to interact with the bone remodeling cascade, by combining them with a calcium phosphate substrate. Calcium phosphates (CaP) are ideal candidates to support bone regeneration, mainly because they possess a close resemblance to the mineral phase of bone, i.e. hydroxyapatite (HA). We have recently proved the osteoimmunomodulatory properties of heparinized CaP (Diez-Escudero et al., 2018). Recent studies have also shown enhanced biological interactions in the presence of heparin immobilized on collagen or CaPs matrices cultured with fibroblast, endothelial and mesenchymal stem cells (König et al., 2014; Lode et al., 2008).

Despite CaPs exhibit good performance as bone graft materials *in vitro* and *in vivo*, one of their main drawbacks is their poor resorption rate. Hence, promoting their resorption is fundamental for the replacement of bone grafts by new bone. Nevertheless, such a strategy would not be advised to patients suffering from osteoporosis due to the inherently high osteoclastic activity. The aim of the present study was to use heparin as a tool to tune the initial inflammatory response and osteoclastogenesis evoked by a CaP, which are crucial events in the early stages of bone remodeling. The effect of heparin functionalization on calcium deficient hydroxyapatite (CDHA) was analyzed using primary human cells to closely resemble the clinical scenario of bone grafts. A widely known synthetic bone graft, β-tricalcium phosphate (β-TCP) was used as a control, together with tissue culture polystyrene (TCPS).

2. Materials and Methods

2.1. Materials: characterization and functionalization

CDHA was obtained by hydrolysis of α-tricalcium phosphate (α-TCP). α-TCP was produced by a solid state reaction at 1400 °C of calcium hydrogen phosphate (CaHPO4, Sigma-Aldrich, St. Louis, USA) and calcium carbonate (CaCO3, Sigma-Aldrich, St. Louis, USA) at a 2:1 molar ratio for 15 h and then quenched in air. The α-TCP was milled to a final median size of 5.2 µm (Espanol et al., 2009). α-TCP containing 2 wt.% of precipitated HA (PHA, Merck KGaA, Darmstadt, Germany) was mixed with a liquid phase consisting of distilled water at a liquid to powder (L/P) ratio of 0.35 mL/g, resulting in a paste that was transferred into PTFE moulds to fabricate discs of either 15 mm diameter x 2 mm thickness or 5 mm diameter x 1 mm thickness. The discs were left to set at 37 °C for 10 days in water to allow for complete hydrolysis to CDHA. β-TCP discs were obtained by sintering the previously obtained CDHA discs at 1100 °C for 9 h and cooling down in air.

Phase identification was performed by XRD (Bruker, Cu Kα, 40 kV, 40 mA). Data were collected in 0.02° steps over the 2θ range of 10°-80° with a counting time of 2 s per step. The experimental patterns were compared to those of hydroxyapatite (JCPDS 09-0432), α-TCP (JCPDS 09-0348) and β-TCP (JCPDS 09-0169). Phase quantification was performed using EVA software (DIFFRAC.EVA software, Bruker) based on reference intensity ratio (RIR). Pore size distribution was investigated by mercury intrusion porosimetry (MIP, Autopore IV Micromeritics), by recording intrusion-extrusion curves from 30 to 30000 psia. The specific surface area (SSA) was assessed by nitrogen adsorption using the BET method (ASAP 2020, Micromeritics). Finally, the microstructure of the substrates was investigated by scanning electron microscopy (SEM, FIB Zeiss Neon40).

Heparin immobilization was performed through an amidation reaction using a first step of silanization with aminopropyltrietoxysilane (APTES, Sigma-Aldrich, St. Louis, USA) followed by 1-(3-dimethylaminoporpyl)-3-ethylcarbodiimide (EDC, Sigma-Aldrich, St. Louis, USA) and N-hydrosuccinimide (NHS, Sigma-Aldrich, St. Louis, USA) adapted from literature (Williams, 2014) to couple heparin by its carboxyl groups. CDHA discs (2x15 mm2) were immersed overnight in absolute ethanol solution with 2 %v/v APTES and 3 %v/v distilled water under agitation at 100 rpm, in order to obtain aminated surfaces. Afterwards, the discs were rinsed in absolute ethanol and sonicated for 5 minutes to remove unbound heparin. Subsequently, heparin solutions with different concentrations (50, 100, 150, 250, 500 and 1000 μg/mL) were prepared. Heparin was dissolved in phosphate buffered saline (PBS, Gibco) and activated by reducing the pH to 6.5 by the addition of hydrochloric acid (HCl, 0.1 M) for 15 minutes in the presence of EDC/NHS. Immediately afterwards, pH was raised using sodium hydroxide (NaOH, 0.1 M) to 7.5, and 1 mL of activated heparin solution was poured onto the aminated discs and left under agitation for 2 h for coupling. Supernatants were collected and the concentration of heparin was determined through an indirect colorimetric method based on

toluidine blue, adapted from the literature (Ahola et al., 2001). Finally, the heparinized discs (CDHA-H) were rinsed in PBS and sonicated for 5 minutes in order to remove non-covalently attached heparin.

2.2. Inflammatory response

Monocytes and neutrophils were isolated in a two-step procedure from human buffy coats from volunteer donors at Uppsala University Hospital. Briefly, for monocyte isolation, 15mL of human blood diluted in PBS (1:1) was layered onto Ficoll-Paque Plus (GE Healthcare) and monocytes were isolated by density gradient centrifugation. The upper plasma layer was collected and stored at 4 °C for later use. The mononuclear ring was collected and washed 3 times with PBS. Cells were resuspended in PBS and counted by exclusion method using Trypan blue (1:5) in a cytometer. Neutrophils underwent a second separation step using 20 mL of 3% dextran in 0.9% saline solution. After 25 minutes, the supernatant was centrifuged and treated with 0.2% saline solution for 20 seconds to remove erythrocytes. The cell suspension was further centrifuged, resuspended in PBS, and a solution containing 6 wt.% acetic acid was used to count cells in a cytometer.

Both cell types were diluted in cell culture media (4PBS/1RPMI-1640/100mM glucose) at a density of $1 \cdot 10^6$ cells/mL. Prior to seeding, 5x1 mm^2 discs were placed in 96 white opaque well plates (Perkin Elmer) and sterilized with 70% ethanol for 3 hours, followed by thrice rinsing with PBS for 15 minutes each prior to cell seeding. 200 µL of cells were added to the discs, immediately followed by the addition of 100 µL of luminol solution (500 µM). Cells were activated with 1 µM phorbol-12-myristate-13-acetate (PMA, Sigma Aldrich), while cells placed onto TCPS without any PMA stimulation were used as a negative control.

Luminol-amplified chemiluminescence was used to study the inflammatory response of cells in contact with the discs (5×1 mm^2) by monitoring the release of reactive oxygen species over a period of 2 hours. Luminol solution was prepared from stock solution (50 mM of luminol in 0.2 M NaOH) mixing 1% luminol stock and 0.2% horseradish peroxidase (1 mg/mL). For the plasma-containing studies, 10% of human plasma was added to the cell medium. Luminescence was monitored at 37 °C every 2 min over 2 hours, as previously described (Mestres et al., 2015). Triplicates for each material were used and the experiment was repeated twice with independent buffy coats for each cell type.

2.3. Culture of osteoclast precursor (OCP) cells

Peripheral blood mononuclear cells (PBMC), containing the precursors of human osteoclasts (OCP), were isolated from buffy coats of healthy voluntary blood donors to the National Blood Transfusion Service. Donation was anonymous, and institutional review board (IRB) approval was not required. Density centrifugation with Ficoll-Histopaque gradient (Sigma–Aldrich) was used to isolate the mononuclear cells as earlier described (Ciapetti et al., 2017). Cells were resuspended in Dulbecco's Modified Eagle's Medium–High Glucose (DMEM, Euroclone, Milan, Italy) supplemented with 10% fetal bovine serum (FBS, Euroclone) and 1% Penicillin/Streptomycin, to provide the complete DMEM. CDHA, CDHA-H, β-TCP and TCPS were sterilized using 70% ethanol for 3h, followed by three rinses with PBS for 15 min each. Complete medium was added after the sterilization and kept overnight prior to cell seeding, as preconditioning treatment to minimize ionic exchange.

Mononuclear cells were resuspended in complete DMEM and seeded on discs and TCPS at a density of $6 \cdot 10^6$ cells/cm^2 and $3 \cdot 10^6$ cells/cm^2, respectively. After 2 h of incubation, non-adherent cells were gently removed and complete DMEM supplemented with 25%

osteoblast supernatant (differentiation medium). As previously reported (Avnet et al. 2011), osteoblast supernatant contains RANKL, and has been proven as differentiation medium yielding similar results as those with supplementation of recombinant RANKL and M-CSF (Granchi et al. 2004). Cell cultures were performed up to 28 days and differentiation medium was refreshed every 3 days.

2.3.1. OCP morphology

Osteoclast morphology at 14, 21 and 28 days of culture was investigated by SEM (FIB Zeiss Neon40). At each time point, cells were rinsed with PBS and fixed using 2% paraformaldehyde/2% glutaraldehyde in 0.1 M cacodylate buffer overnight at 4 °C. Afterwards, samples were dehydrated in ethanol and dried. A thin carbon layer was sputtered prior to imaging to impart conductivity to samples.

Tartrate-resistant acid phosphatase and Hoechst 33258 staining (TRAP-Hoechst, Sigma Aldrich) at 14, 21 and 28 days was used to study OC morphology and differentiation. At each time point, cells were fixed using 3% paraformaldehyde-2% sucrose for 30 min. Afterwards, the cell membrane was permeabilized with Triton 0.5% in 4-(2-hydroxyethyl)-1-piperazineethanesulfonic acid (HEPES) for 5 min at room temperature, and finally stained using naphthol AS-BI phosphoric acid and tartrate solution (Acid Phosphatase kit, Sigma–Aldrich) for 60 min at 37 °C for the cytoplasm and 2.25 µg/mL of Hoechst 33258 for 10 min in the dark for the nuclei. TRAP-Hoechst stained samples were analyzed by fluorescence microscopy at 360 nm excitation and 470 nm emission. ImageJ software was used to perform a semi-quantitative analysis of the multinucleated cells found by optical microscopy. Duplicates of 5x1 mm^2 material discs and duplicates of plastic chamber-slides as controls were used for the morphological study.

2.3.2. OC activity

In order to assess the OC differentiation, tartrate-resistant acid phosphatase (TRAP) activity was quantified both in cell lysates and culture supernatants at the end of the culture (28 days). Briefly, cells grown on the material substrates were rinsed in PBS and lysed with 0.1% Triton X-100/1 M NaCl (Sigma-Aldrich). 50 µL of the cell lysate was transferred to a new plate and 50 µL 4-nitrophenyl phosphate (4.61 mg/mL)/40 mM Na-tartrate/50 mM Na-acetate (pH 4.8) were added. After 1 hour incubation at 37 °C, the reaction was stopped with 50 µL of sodium hydroxide (NaOH, 0.2M), and the absorbance was measured at 405 nm in a spectrophotometer (Infinite F200 Pro Microplate Reader; TECAN, Mannedorf, Switzerland). Bicinchoninic acid colorimetric assay (BCA, Pierce BCA Protein Assay Kit, Rockford, USA) was used to quantify the total protein in lysates according to the manufacturer's instructions. Material substrates without cells (blank) were measured and subtracted from cell-seeded materials. TRAP activity was then normalized to the total protein content after blank subtraction.

Tartrate-resistant acid phosphatase isoform 5b (TRAP5b) concentration was investigated after 28 days of culture. Cell supernatants were collected, centrifuged at 400g for 5 min and assayed using the BoneTRAP® Assay kit (Pantec S.r.l., Torino, Italy), according to the manufacturer's instructions. The concentration of TRAP5b protein in the supernatants was determined by reading the absorbance at 405 nm in the spectrophotometer. Data are expressed as the mean concentration (units/liter) after subtraction of the corresponding cell-free readout.

Calcium release and pH were monitored over cell culture time at 0, 3, 7, 14, 21 and 28 days. At each time point, the supernatants were collected, centrifuged at 2800 rpm for 5 minutes and kept at 4°C until measurement. Calcium release was measured using a colorimetric method based on ortho-cresolphthalein complexone (OCPC, Sigma-

Aldrich) adapted from literature (Sariibrahimoglu, Leeuwenburgh, Wolke, Yubao, & Jansen, 2012). The absorbance was measured at 570 nm using a UV-vis spectrophotometer (Infinite M200 Pro Microplate Reader; TECAN, Manndorf, Switzerland). The pH value was measured using a pH-meter (MultiMeter MM 41).

2.4. Statistical analyses

Triplicates of 15×2 mm^2 and 5×1 mm^2 material discs were used for all experiments. Data are represented as the mean value $\pm$ standard error of the mean. Data sets for TRAP measurements and multinucleated cell counting were normally distributed (homogeneous variance, Levene> 0.05) and analyzed using one-way ANOVA, with post-hoc Tukey test used to assess significant differences. The data set for the number of nuclei was not normally distributed and non-parametric Kruskal-Wallis was used to assess significant differences. Values of $p < 0.05$ were considered significant. All statistics were performed using IBM® SPSS® Statistics 24 software.

3. Results

3.1. Materials characterization

Phase composition as measured by XRD (Figure 1A) showed that CDHA consisted of a poorly crystalline hydroxyapatite phase (JCPDS 09-0432), as indicated by the broad peaks. A small amount of unreacted α-TCP was detected (JCPDS 09-0348), accounting for 2 wt.%, as quantified by EVA Software. β-TCP samples were phase-pure and showed the sharp peaks typical of crystalline sintered materials (JCPDS 09-0169).

According to MIP analysis (Figure 1B), CDHA exhibited a broad pore size distribution ranging from 10 to 100 nm. In contrast, β-TCP specimens presented larger pores, centered around 1 µm, although they also exhibited some nanoporosity. The total

porosity was similar for both substrates (Figure 1C), but the microstructure of the two ceramic substrates was clearly different. Whereas CDHA consisted of an entangled network of plate-like crystals, β-TCP presented a smooth polyhedral grain microstructure (Figure 1C, a and b), which resulted in very different values of SSA, i.e. 24 m^2/g for CDHA and 0.4 m^2/g for β-TCP. Finally, the results of total heparin immobilization on the substrates are displayed in Figure 1D, together with an inset showing that the plate-like nanostructure of CDHA was preserved after heparin functionalization. The maximum covalent attachment yield was achieved with concentrations above 500 µg/mL, which allowed for the immobilization of approximately 200 µg of heparin on the surface of 2x15 mm^2 diameter discs.

3.2. Inflammatory response

The release of ROS by neutrophils and monocytes activated with PMA in contact with the different substrates is depicted in Figure 2A and B, respectively. The inflammatory response of neutrophils with and without plasma is shown in Figure 2A. CDHA exhibited the lowest ROS release among all substrates either with or without plasma, followed by CDHA-H and β-TCP. All PMA-stimulated substrates showed a peak within the first 5 min. Plasma-containing samples showed a slight increase in ROS signal compared to samples with an absence of plasma. No release of ROS was observed in the negative control (TCPS) without PMA activation. The values of ROS release by monocytes was slightly higher than that of neutrophils (Figure 2B); however, ROS peaks were shifted to a longer time (20 min). The cells on activated TCPS (TCPS+) showed bimodal ROS release kinetics, with two ROS peaks at 20 and 50 min. Monocytes on biomimetic substrates CDHA and CDHA-H exhibited the lowest ROS signals, approximately 60% and 30%, in the presence and absence of plasma respectively, showing a mean peak at 20 min in all substrates (Figure 2B). The presence of plasma increased the release of ROS for both CDHA and CDHA-

H, though it diminished after 1h to half of its value. No effect of plasma was found for β-TCP, which yielded approximately 70-80% of ROS regardless of the presence or lack of human plasma.

3.3. OCP cells morphology

The evolution of OCP cell morphology was qualitatively evaluated by SEM. Figure 3 shows the cell morphology (purple color) on the different substrates at 14, 21 and 28 days. Round cells were found on TCPS at 14 days, which became bigger and more spread after 21 and 28 days. At 28 days, protuberances surrounded by a flat halo were visible for all cells, compatible with mature OC morphology. The β-TCP substrate showed a high number of round cells at 14 days, which spread and showed several connecting filopodia at 21 and 28 days. Biomimetic substrates, CDHA and CDHA-H, also supported OC adhesion as shown in the images at 14 days. After 21 days, cells on CDHA-H appeared more elongated than on CDHA, and at 28 days the presence of cell clusters was observed in some regions of the samples, particularly on CDHA-H surfaces. Higher magnification images of the cells on CDHA-H at 28 days (Figure 3m) showed regions with degraded crystals (arrows) compared to the pristine plate-like microstructure of the material (*). This was compatible with OC resorption and was especially evident close to the cells (Figure 3m and n). Figure 3o shows a region totally covered by cells on CDHA-H. A higher magnification image (Figure 3p) displays degraded plate-like crystals (arrows) typical of CDHA in the zones adjacent to OC compared to the pristine nanostructure (*).

The differentiation of OCP cells was monitored using TRAP-Hoechst staining at each time point (14, 21 and 28 days). Fewer adherent cells were observed on the biomimetic substrates compared to sintered β-TCP. At 14 days, multinucleated cells were evident only on TCPS and CDHA-H (Figure 4D and J, black arrows). This aspect was

maintained over 21 and 28 days for both substrates (Figure 4E and F for CDHA-H, and Figure 5K and L for TCPS). Only at 28 days were some multinucleated cells found on CDHA and β-TCP (Figure 4C and Figure 4I, respectively), even if few cell clusters were visible already at 14 and 21 days for CDHA (Fig. 4A and B).

Image analyses based on the TRAP-Hoechst optical images allowed quantitative information to be obtained and were used to disclose the cell behavior on the different substrates (Figure 4M). A high number of multinucleated cells were found on TCPS at 14 days, which increased with time (21 and 28 days). CaP substrates hosted a lower number of multinucleated cells compared to TCPS. For CDHA, the presence of heparin (CDHA-H) resulted in a higher number of multinucleated cells at all-time points, whereas β-TCP and pristine CDHA showed a lower number of multinucleated cells. A more in-depth study on the morphology of the multinucleated cells revealed different fusion patterns over time. Figure 4N shows the prevalent cells with different numbers of nuclei. The substrates hosting the highest number of multinucleated cells, i.e. CDHA-H and TCPS, showed also a higher number of cells with 3 to 5 or 6 to 10 nuclei regardless of time, compatible with OC maturation.

3.3. OC activity

To assess the osteoclastic differentiation of OCP, TRAP activity was assessed on both culture supernatants and cells, the last normalized to the total protein content. Figure 5A shows the total protein in the cell lysates at 28 days. Heparinized CDHA-H showed the highest protein content, followed by CDHA and β-TCP, with TCPS scoring the lowest protein content. Similar levels of TRAP activity normalized to the protein content were observed for the OCP cells cultured on the different CaP substrates, all of them significantly lower than the values found for the cells cultured on TCPS (Figure. 5B). The presence of heparin resulted in a decrease of TRAP activity, although the difference

with the pristine CDHA was not statistically significant. Moreover, TRAP5b, an active enzyme released by differentiated OC capable of degrading bone matrix proteins was investigated in culture supernatants after 28 days. Analogously to what was found for TRAP activity, the concentration of the TRAP5b isoform released by the cells cultured on the CaP substrates was lower than that of the cells cultured on the control TCPS, and similar for all the materials (Figure 5C).

Osteoclast activity can also be analyzed in terms of substrate degradation and the consequent calcium release and pH change due to the resorptive activity of OC. Figure 6A represents the Ca^{2+} concentration in the cell culture medium at each time point. The highest Ca^{2+} concentration was registered when OC precursors were cultured on β-TCP. Both biomimetic substrates were found to subtract calcium from the medium with time, showing similar Ca^{2+} values irrespective of heparin functionalization (Figure 6B). Yet, in presence of cells, the concentration of Ca^{2+} in the culture medium increased in all substrates. In contrast, the cell culture medium showed a slight decrease of pH in the presence of cells for all substrates, which was more pronounced on the CaP substrates, especially at early time points (Figure 6C). The variation of pH comparing cells vs. no cells showed higher acidification for CDHA-H and β-TCP maintained over time (Figure 6D).

4. Discussion

The initial cellular responses that follow biomaterial implantation are firstly modulated by the ROS release activating signal transduction pathways (Loi et al., 2016). CaP ceramics, such HA and β-TCP are known to evoke a consistent inflammatory cell response when tested as particles or following the resorption of calcium-containing biomaterials (Velard, Braux, Amedee, & Laquerriere, 2013). In addition, the topography

of CaP has also been shown to play a major role in inflammation (Mestres et al., 2015). Recently, some authors explored the immune response to GAGs claiming an anti-inflammatory effect of particular GAGs, such as heparin (Ting et al., 2013; Zhou, Niepel, Saretia, & Groth, 2016). This was not confirmed in the present study, since, in fact, lower ROS levels were recorded when monocytes and neutrophils were cultured on pristine CDHA compared to CDHA-H. In addition, the anti-oxidant effect of human plasma, attributed to the scavenging role of proteins, mainly albumin, was not observed (Das et al., 2017). Although the neutrophil response was not particularly affected by the presence of plasma, monocytes presented the opposite trend, with lower percentages of ROS in the absence of plasma (Figure 2B). Among the different CaP substrates, biomimetic CDHA and CDHA-H induced the lowest ROS release under PMA activation, irrespective of the presence or not of heparin (Figure 2A and B), which confirms that no specific response was activated upon monocyte or neutrophil contact with heparin. Sintered β-TCP yielded the higher oxidative stress among all CaP substrates, in agreement with previous results (Yamada, Minamikawa, Ueno, Sakurai, & Ogawa, 2012).

Three main molecules play pivotal roles in the OC maturation from OCP or macrophages, RANKL, OPG and M-CSF (Teitelbaum, 2000) which are secreted by stromal cells and osteoblasts. The balance RANKL and OPG, a decoy receptor that competes with RANK for RANKL, usually dictates osteoclastogenesis. Inhibition of osteoclastogenesis occurs when OPG binds to RANKL; on the contrary, stromal cells and osteoblasts can secrete higher doses of RANKL to enhance bone resorption.

One of the limiting factors of hydroxyapatite is its poor resorbability. Hence, our hypothesis was that heparin functionalization could be used to enhance osteoclast formation and the cell-mediated resorption of apatitic substrates, by acting on the

RANKL/OPG balance. Previous studies have shown that direct supplementation of heparin in the cell culture media interfered with OPG, leaving higher amounts of RANKL available for OC maturation (Lamoureux, Baud'huin, Duplomb, Heymann, & Rédini, 2007, Irie et al., 2007). This hypothesis was tested by culturing primary human osteoclast precursor cells on the surface of a biomimetic CDHA covalently functionalized with heparin (CDHA-H), and comparing the cell response with that on pristine CDHA and a more resorbable CaP such as β-TCP. Covalent immobilization was preferred in order to discard any possible effects from heparin release during cell cultures. Upon grafting, sonication and three rinsing steps were performed to remove unbound heparin prior to cell studies. Quantification of heparin in the rinses prove that above 80% of the heparin remained firmly attached (data not shown).

Although the present work has limitations regarding the full assessment of OC phenotype, the effect of heparin was clearly demonstrated by TRAP-Hoechst staining (Figure 4). Even if macrophage fusion and OC formation was lower in number on CaP substrates than on control TCPS, the presence of heparin (CDHA-H, Figure 4D, E, F) significantly increased the number of multinucleated cells compared to pristine CDHA or β-TCP (Figure 4A, B, C and Figure 4G, H, I, respectively). A relevant measure to conclude the OPG sequestering effect due to the heparin and hence confirm the pro-osteoclastogenic effect is to investigate the possible uptake of RANKL-OPG by heparinized substrates at both the beginning and the end of cell studies. Another important aspect that has to be further investigated is whether the substrates could lead to the formation of foreign body giant cells (FBGC), which are related to OCs and are also multinucleated cells. FBGCs are usually TRAP-positive, but nevertheless they possess higher number of nuclei (>10) (ten Harkel et al., 2015). The formation of multinucleated cells with less than 10 nuclei was evident on all substrates, except for β-

TCP at 14 days (Figure 4M). Multinucleated cells (>3 nuclei) were found on CDHA-H at 14 days (Figure 4D), while on the pristine substrates similar OCs were found only after 21 or 28 days (Figure 4B and C), and in smaller amounts. Sintered β-TCP and CDHA had similar number of OCs formed at 28 days (Figure 4I and C, respectively). Overall, the presence of heparin on CDHA-H resulted in an enhancement of osteoclastogenesis, similar to TCPS although the cell number was smaller, probably due to the CDHA roughness, which might hamper cell adhesion. Maturation of OC on HA substrates after 10 to 13 days has been reported, showing preferential differentiation of rat bone marrow cells on nanostructured alumina and HA compared to microstructured surfaces (Webster, 2001). Other authors have pointed to a preferential OC maturation on smooth surfaces, due to disruption of OC actin sealing zones on rougher surfaces (Costa et al., 2013). Likewise, an increase in the surface area, microporosity and wettability of biomaterial surface has been reported to decrease OC differentiation and function, compared to microsized grain topography (Costa-Rodrigues, Carmo, Perpétuo, Monteiro, & Fernandes, 2016).

Recently, in a previous work, we demonstrated that rough surfaces, such as biomimetic CDHA with different nanotopographies, were permissive for OC formation after 21 days (Ciapetti et al., 2017). Even if no resorption pits were clearly evident from SEM analysis in similar materials, early stages of OC activity were detected using focused ion beam (FIB) to transversally section the cells and the underlying substrate (Diez-Escudero et al., 2017). Likewise, in the present study, although it was difficult to identify resorption pits on the CaP substrates (Figure 3), after 28 days of culture, degraded regions were found in the vicinity of cells (Figure 3m-p), compatible with OC resorptive activity, as observed in previous studies (Leeuwenburgh et al., 2001; Schilling et al.,

2004). Both authors found morphological changes in the microstructure of their substrates upon contact with OC.

Besides multinuclearity, TRAP activity and TRAP5b release by OC were also investigated after 28 days. No conclusive information can be drawn from both analyses since no significant differences were found among the different CaP substrates (Figure 5). Since cell fusion was already detected after 14 days for CDHA-H or 21 days for the other CaP substrates, one possible explanation could be that 28 days was too late a time point, with the peak of TRAP5b expression occurring earlier. Remarkable differences in TRAP and TRAP5b were noticed only when CaP substrates were compared to TCPS. These results also suggest that additional studies to conclusively support the effect of heparin on improved osteoclastogenesis are required, such as osteoclastic markers by gene expression. However, sulfated GAGs have been reported to strongly interfere in RNA to DNA preparations (Salbach et al., 2012), and alternative methods might be required.

Indirect information on OC activity can be inferred from the extracellular calcium and pH measurements, both being parameters indicative of OC activity (Schilling et al., 2004). Osteoclastic resorption of the substrate should lead to an increase in Ca^{2+} concentration in the culture medium. However, this can be masked by the variations in calcium merely caused by the interaction of the culture medium with the CaP substrates, even with the absence of cells. The CaPs analyzed in this study are prone to uptake of calcium from cell culture medium, especially CDHA (Sadowska, Guillem-Marti, Montufar, Espanol, & Ginebra, 2017). Due to this inherent uptake, the evaluation of OC activity on such substrates can be tricky. Nevertheless, CDHA and CDHA-H in the presence of cells showed a reduction in the calcium uptake, compatible with the resorption activity of OC. The increase in Ca^{2+} concentration was more marked for β-

TCP (Figure 6A, B), which could be related to its higher solubility compared to CDHA. Additionally, an acidification of the cell culture medium, which is related to OC activity (Kato & Morita, 2013), was found for all CaP substrates in the presence of cells, compared to TCPS (Figure 6D). β-TCP showed the highest pH variations, followed by CDHA-H, which were maintained over the time points of the experiment.

Overall, the presence of a high number of multinucleated cells on CDHA-H indicates that heparin plays an important role as an osteoclastogenesis modulator in primary human cells. Additionally, SEM images supported the OC activity as evidenced by the degraded microstructures adjacent to the cells. In agreement with literature (Lamoureux et al., 2007), we hypothesize that the effect of heparin on OC maturation could be due to changes the OPG/RANKL balance.

These findings, coupled with the recently reported osteoimmunomodulatory effect of heparinized surfaces on MSC differentiation (Diez-Escudero et al., 2018), support the development of heparin-mimicking materials as a tool to promote the integration of regenerative bone graft materials in the bone remodeling process, with minimal inflammatory responses and enhanced cellular signaling.

5. Conclusions

Despite the fact that heparin functionalization of biomimetic CDHA could not downregulate ROS release, which was already low on nanostructured CDHA compared to sintered microstructured β-TCP, heparin was shown to selectively stimulate human OCP cells fusion and maturation. Early OC maturation was demonstrated on heparinized substrates at 14 days, which was believed to be the reason for the low activity registered for TRAP and TRAP5b at 28 days. SEM analyses further confirmed

the presence of degraded regions on heparinized CDHA as a result of OC activity. Overall, this study demonstrates the enhancement of osteoclastogenesis due to the presence of heparin on biomimetic CDHA. This strategy represents a promising tool to help integrate biomaterials in the bone remodeling cycle. Nevertheless, the overall effect of heparin on osteoclastogenesis should be further tested by analyzing the OC phenotype, and consequently followed by *in vivo* studies.

Author contribution

The work was conceived and supervised by A. Diez-Escudero, G. Ciapetti, N. Baldini, C. Persson, M. Espanol and M.-P. Ginebra. A. Diez-Escudero synthesized and characterized the materials under the supervision of M. Espanol and M.-P. Ginebra. A. Diez-Escudero and M. Espanol carried out heparin functionalization and optimization. A. Diez-Escudero carried out the biological studies corresponding to inflammation under C. Persson and M.-P. Ginebra supervision; A. Diez-Escudero, E. Torreggiani and G. Di Pompo perfomed all the osteoclasts studies under the supervision and guidance of

G. Ciapetti, N.Baldini and M.-P. Ginebra. A. Diez-Escudero edited the manuscript with collaboration of all authors. All authors discussed the data and revised the manuscript at all stages.

Conflicts of interest

The authors declare no competing financial interests.

References

Ahola, M. S., Säilynoja, E. S., Raitavuo, M. H., Vaahtio, M. M., Salonen, J. I., & Yli-Urpo, A. U. O. (2001). In vitro release of heparin from silica xerogels. *Biomaterials*, *22*(15), 2163–2170. https://doi.org/10.1016/S0142-9612(00)00407-5

Anderson, J. M., Rodriguez, A., & Chang, D. T. (2008). Foreign body reaction to biomaterials. *Seminars in Immunology*, *20*(2), 86–100. https://doi.org/10.1016/j.smim.2007.11.004

Avnet, S., Pallotta, R., Perut, F., Baldini, N., Pittis, M. G., Saponari, A., … Lattanzi, G. (2011). Osteoblasts from a mandibuloacral dysplasia patient induce human blood precursors to differentiate into active osteoclasts. *Biochimica et Biophysica Acta - Molecular Basis of Disease*, *1812*(7), 711–718. https://doi.org/10.1016/j.bbadis.2011.03.006

Bramono, D. S., Murali, S., Rai, B., Ling, L., Poh, W. T., Lim, Z. X., … Cool, S. M. (2012). Bone marrow-derived heparan sulfate potentiates the osteogenic activity of bone morphogenetic protein-2 (BMP-2). *Bone*, *50*(4), 954–964. https://doi.org/10.1016/j.bone.2011.12.013

Capila, I., & Linhardt, R. J. (2002). Heparin-protein interactions. *Angewandte Chemie (International Ed. in English)*, *41*(3), 391–412. Retrieved from http://www.ncbi.nlm.nih.gov/pubmed/12491369

Ciapetti, G., Di Pompo, G., Avnet, S., Martini, D., Diez-Escudero, A., Montufar, E. B., … Baldini, N. (2017). Osteoclast differentiation from human blood precursors on biomimetic calcium-phosphate substrates. *Acta Biomaterialia*, *50*, 102–113. https://doi.org/10.1016/j.actbio.2016.12.013

Costa-Rodrigues, J., Carmo, S., Perpétuo, I. P., Monteiro, F. J., & Fernandes, M. H. (2016). Osteoclastogenic differentiation of human precursor cells over micro- and nanostructured hydroxyapatite topography. *Biochimica et Biophysica Acta (BBA) - General Subjects*, *1860*(4), 825–835. https://doi.org/10.1016/j.bbagen.2016.01.014

Costa, D. O., Prowse, P. D. H., Chrones, T., Sims, S. M., Hamilton, D. W., Rizkalla, A. S., & Dixon, S. J. (2013). The differential regulation of osteoblast and osteoclast activity by surface topography of hydroxyapatite coatings. *Biomaterials*, *34*(30), 7215–7226. https://doi.org/10.1016/j.biomaterials.2013.06.014

Das, S., Maras, J. S., Hussain, M. S., Sharma, S., David, P., Sukriti, S., … Sarin, S. K. (2017). Hyperoxidized albumin modulates neutrophils to induce oxidative stress and inflammation in severe alcoholic hepatitis. *Hepatology*, *65*(2), 631–646. https://doi.org/10.1002/hep.28897

Diez-Escudero, A., Espanol, M., Bonany, M., Lu, X., Persson, C., & Ginebra, M.-P. (2018). Heparinization of Beta Tricalcium Phosphate: Osteo-immunomodulatory Effects. *Advanced Healthcare Materials*, *7*(5), 1700867. https://doi.org/10.1002/adhm.201700867

Diez-Escudero, A., Espanol, M., Montufar, E. B., Di Pompo, G., Ciapetti, G., Baldini, N., & Ginebra, M.-P. (2017). Focus Ion Beam/Scanning Electron Microscopy Characterization of Osteoclastic Resorption of Calcium Phosphate Substrates. *Tissue Engineering Part C: Methods*, *23*(2), 118–124. https://doi.org/10.1089/ten.tec.2016.0361

Espanol, M., Perez, R. A., Montufar, E. B., Marichal, C., Sacco, A., & Ginebra, M. P. (2009).

Intrinsic porosity of calcium phosphate cements and its significance for drug delivery and tissue engineering applications. *Acta Biomaterialia*, *5*(7), 2752–2762. https://doi.org/10.1016/j.actbio.2009.03.011

Franz, S., Rammelt, S., Scharnweber, D., & Simon, J. C. (2011). Immune responses to implants – A review of the implications for the design of immunomodulatory biomaterials. *Biomaterials*, *32*(28), 6692–6709. https://doi.org/10.1016/j.biomaterials.2011.05.078

Granchi, D., Amato, I., Battistelli, L., Avnet, S., Capaccioli, S., Papucci, L., … Baldini, N. (2004). In vitro blockade of receptor activator of nuclear factor-κB ligand prevents osteoclastogenesis induced by neuroblastoma cells. *International Journal of Cancer*, *111*(6), 829–838. https://doi.org/10.1002/ijc.20308

Granchi, D., Amato, I., Battistelli, L., Ciapetti, G., Pagani, S., Avnet, S., … Giunti, A. (2005). Molecular basis of osteoclastogenesis induced by osteoblasts exposed to wear particles. *Biomaterials*, *26*(15), 2371–2379. https://doi.org/10.1016/j.biomaterials.2004.07.045

Gschwandtner, M., Strutzmann, E., Teixeira, M. M., Anders, H. J., Diedrichs-Möhring, M., Gerlza, T., … Kungl, A. J. (2017). Glycosaminoglycans are important mediators of neutrophilic inflammation in vivo. *Cytokine*, *91*, 65–73. https://doi.org/10.1016/j.cyto.2016.12.008

Hempel, U., Preissler, C., Vogel, S., Möller, S., Hintze, V., Becher, J., … Dieter, P. (2014). Artificial extracellular matrices with oversulfated glycosaminoglycan derivatives promote the differentiation of osteoblast-precursor cells and premature osteoblasts. *BioMed Research International*, *2014*, 938368. https://doi.org/10.1155/2014/938368

Hintze, V., Moeller, S., Schnabelrauch, M., Bierbaum, S., Viola, M., Worch, H., & Scharnweber, D. (2009). Modifications of Hyaluronan Influence the Interaction with Human Bone Morphogenetic Protein-4 (hBMP-4). *Biomacromolecules*, *10*(12), 3290–

3297. https://doi.org/10.1021/bm9008827

Irie, A., Takami, M., Kubo, H., Sekino-Suzuki, N., Kasahara, K., & Sanai, Y. (2007). Heparin enhances osteoclastic bone resorption by inhibiting osteoprotegerin activity. *Bone*, *41*(2), 165–174. https://doi.org/10.1016/j.bone.2007.04.190

Kato, K., & Morita, I. (2013). Promotion of osteoclast differentiation and activation in spite of impeded osteoblast-lineage differentiation under acidosis: Effects of acidosis on bone metabolism. *BioScience Trends*. https://doi.org/10.5582/bst.2013.v7.1.33

König, U., Lode, A., Welzel, P. B., Ueda, Y., Knaack, S., Henß, A., … Gelinsky, M. (2014). Heparinization of a biomimetic bone matrix: integration of heparin during matrix synthesis versus adsorptive post surface modification. *Journal of Materials Science. Materials in Medicine*, *25*(3), 607–621. https://doi.org/10.1007/s10856-013-5098-8

Lamoureux, F., Baud'huin, M., Duplomb, L., Heymann, D., & Rédini, F. (2007). Proteoglycans: key partners in bone cell biology. *BioEssays*, *29*(8), 758–771. https://doi.org/10.1002/bies.20612

Leeuwenburgh, S., Layrolle, P., Barrre, F., De Bruijn, J., Schoonman, J., Van Blitterswijk, C. A., & De Groot, K. (2001). Osteoclastic resorption of biomimetic calcium phosphate coatings in vitro. *Journal of Biomedical Materials Research*, *56*(2), 208–215. https://doi.org/10.1002/1097-4636(200108)56:2<208::AID-JBM1085>3.0.CO;2-R

Ling, L., Murali, S., Stein, G. S., van Wijnen, A. J., & Cool, S. M. (2010). Glycosaminoglycans modulate RANKL-induced osteoclastogenesis. *Journal of Cellular Biochemistry*, *109*(6), 1222–1231. https://doi.org/10.1002/jcb.22506

Lode, A., Reinstorf, A., Bernhardt, A., Wolf-Brandstetter, C., König, U., & Gelinsky, M. (2008). Heparin modification of calcium phosphate bone cements for VEGF functionalization. *Journal of Biomedical Materials Research. Part A*, *86*(3), 749–759.

https://doi.org/10.1002/jbm.a.31581

Loi, F., Córdova, L. A., Pajarinen, J., Lin, T. hua, Yao, Z., & Goodman, S. B. (2016, May). Inflammation, fracture and bone repair. *Bone*. https://doi.org/10.1016/j.bone.2016.02.020

Mestres, G., Espanol, M., Xia, W., Persson, C., Ginebra, M.-P., & Ott, M. K. (2015). Inflammatory Response to Nano- and Microstructured Hydroxyapatite. *PLOS ONE*, *10*(4), e0120381. https://doi.org/10.1371/journal.pone.0120381

Sadowska, J.-M., Guillem-Marti, J., Montufar, E. B., Espanol, M., & Ginebra, M.-P. (2017). Biomimetic Versus Sintered Calcium Phosphates: The In Vitro Behavior of Osteoblasts and Mesenchymal Stem Cells. *Tissue Engineering Part A*, *23*(23–24), ten.tea.2016.0406. https://doi.org/10.1089/ten.tea.2016.0406

Salbach-Hirsch, J. (2014). Sulfated glycosaminoglycans support osteoblast functions and concurrently suppress osteoclasts. *Journal of Cellular Biochemistry*, *115*(6), 1101–1111. https://doi.org/10.1002/jcb.24750

Salbach, J., Kliemt, S., Rauner, M., Rachner, T. D., Goettsch, C., Kalkhof, S., … Hofbauer, L. C. (2012). The effect of the degree of sulfation of glycosaminoglycans on osteoclast function and signaling pathways. *Biomaterials*, *33*(33), 8418–8429. https://doi.org/10.1016/j.biomaterials.2012.08.028

Sariibrahimoglu, K., Leeuwenburgh, S. C. G., Wolke, J. G. C., Yubao, L., & Jansen, J. a. (2012). Effect of calcium carbonate on hardening, physicochemical properties, and in vitro degradation of injectable calcium phosphate cements. *Journal of Biomedical Materials Research Part A*, *100A*(3), 712–719. https://doi.org/10.1002/jbm.a.34009

Schilling, A. F., Linhart, W., Filke, S., Gebauer, M., Schinke, T., Rueger, J. M., & Amling, M. (2004). Resorbability of bone substitute biomaterials by human osteoclasts. *Biomaterials*, *25*(18), 3963–3972. https://doi.org/10.1016/j.biomaterials.2003.10.079

Severin, I. C., Soares, A., Hantson, J., Teixeira, M., Sachs, D., Valognes, D., … Shaw, J. (2012). Glycosaminoglycan analogs as a novel anti-inflammatory strategy. *Frontiers in Immunology*, *3*(OCT), 293. https://doi.org/10.3389/fimmu.2012.00293

Teitelbaum, S. L. (2000). Bone Resorption by Osteoclasts. *Science*, *289*(5484), 1504–1508. https://doi.org/10.1126/science.289.5484.1504

ten Harkel, B., Schoenmaker, T., Picavet, D. I., Davison, N. L., de Vries, T. J., & Everts, V. (2015). The Foreign Body Giant Cell Cannot Resorb Bone, But Dissolves Hydroxyapatite Like Osteoclasts. *PloS One*, *10*(10), e0139564. https://doi.org/10.1371/journal.pone.0139564

Ting, S. R. S., Whitelock, J. M., Tomic, R., Gunawan, C., Teoh, W. Y., Amal, R., & Lord, M. S. (2013). Cellular uptake and activity of heparin functionalised cerium oxide nanoparticles in monocytes. *Biomaterials*, *34*, 4377–4386. Retrieved from http://www.elsevier.com/copyright

Velard, F., Braux, J., Amedee, J., & Laquerriere, P. (2013). Inflammatory cell response to calcium phosphate biomaterial particles: An overview. *Acta Biomaterialia*, *9*(2), 4956–4963. https://doi.org/10.1016/j.actbio.2012.09.035

Webster, T. (2001). Enhanced osteoclast-like cell functions on nanophase ceramics. *Biomaterials*, *22*(11), 1327–1333. https://doi.org/10.1016/S0142-9612(00)00285-4

Williams, R. L. (2014). *Development of multifunctional calcium phosphate particles for drug delivery and formation of cross-linked materials*. University of Birmingham. Retrieved from http://etheses.bham.ac.uk/5339/

Yamada, M., Minamikawa, H., Ueno, T., Sakurai, K., & Ogawa, T. (2012). N-acetyl cysteine improves affinity of beta-tricalcium phosphate granules for cultured osteoblast-like cells. *Journal of Biomaterials Applications*, *27*(1), 27–36.

https://doi.org/10.1177/0885328210383598

Zhang, Y., Choksi, S., Chen, K., Pobezinskaya, Y., Linnoila, I., & Liu, Z.-G. (2013). ROS play a critical role in the differentiation of alternatively activated macrophages and the occurrence of tumor-associated macrophages. *Cell Research*, *23*(7), 898–914. https://doi.org/10.1038/cr.2013.75

Zhou, G., Niepel, M. S., Saretia, S., & Groth, T. (2016). Reducing the inflammatory responses of biomaterials by surface modification with glycosaminoglycan multilayers. *Journal of Biomedical Materials Research Part A*, *104*(2), 493–502. https://doi.org/10.1002/jbm.a.35587
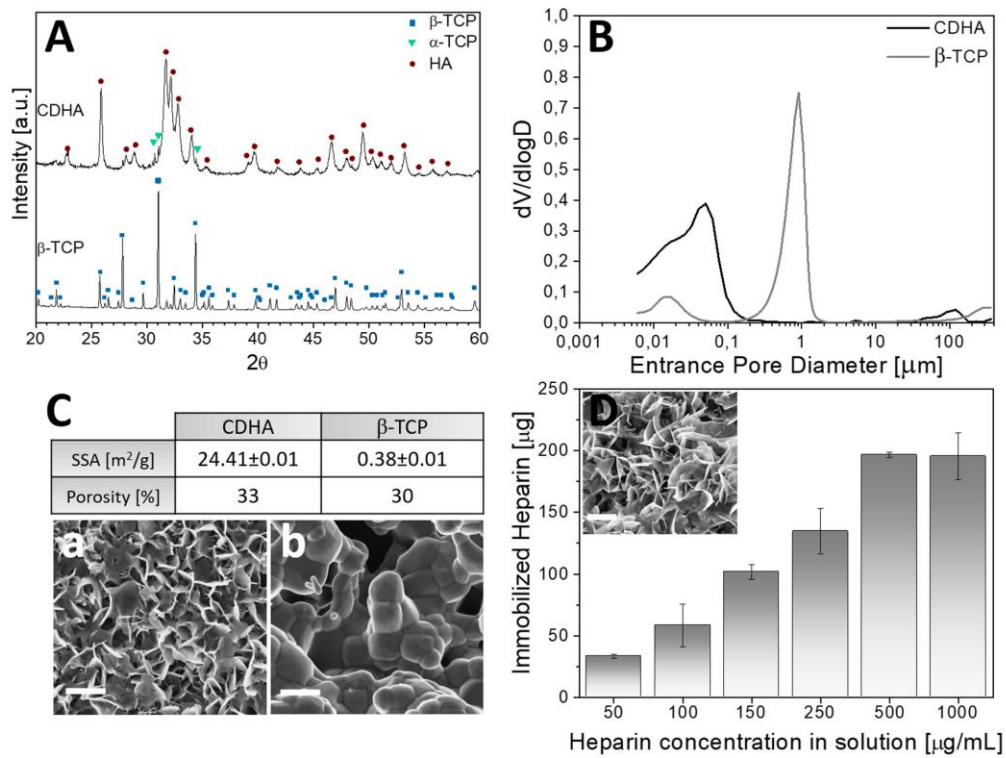
Figure 1. Physicochemical properties of CaP substrates. A: XRD patterns of CDHA and β-TCP; B: pore entrance size distribution; C: Specific surface area (SSA) and porosity values with representative SEM microstructures for CDHA and β-TCP (a and b, respectively, scale bar: 2 µm); D: maximum heparin immobilized on substrate surface (inset: microstructure of heparinized CDHA, scale bar: 2 µm).
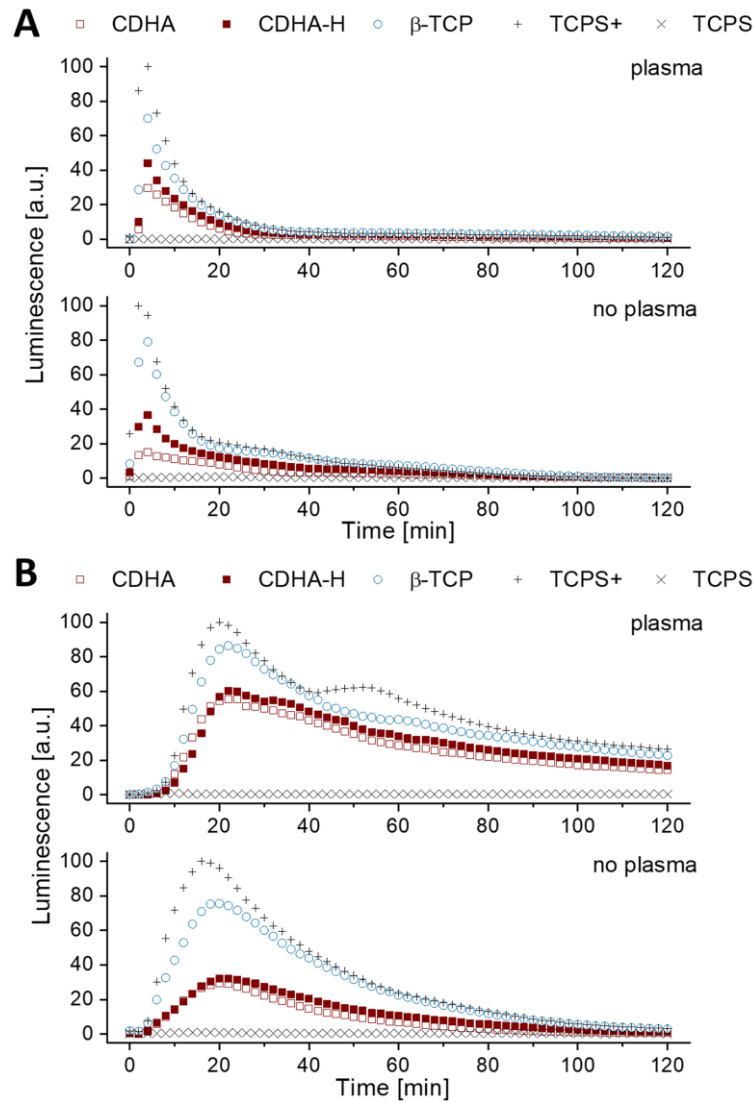
Figure 2. ROS release kinetics of neutrophils (A) and monocytes (B) in contact with substrates over 2 h, in presence of 10% human plasma (top-plasma), and absence (bottom-no plasma).
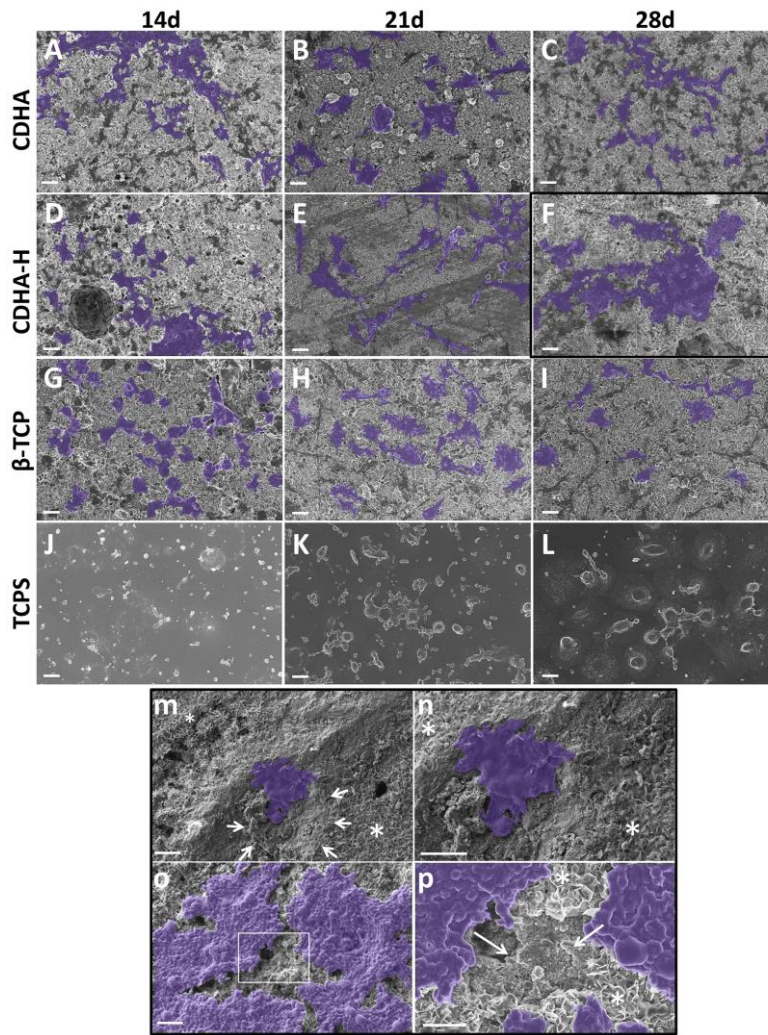
Figure 3. SEM images of osteoclast precursor cells cultured on the substrates at different time points (14 days, first column; 21 days, second column, and 28 days, third column); A, B, C: CDHA; D, E, F: CDHA-H; G, H, I: β-TCP, and J, K, L: TCPS. Scale bar: 20 µm. m-p: Detail of OCP cells on CDHA-H after 28 days of culture, showing Howship lacunae and degraded crystals consistent with OC resorptive activity. m: low magnification image showing a resorption pit (white arrows) with degraded crystals compared to pristine microstructure (*); n: high magnification image showing the resorption area; o: region totally covered by cells; and p: higher magnification image showing degraded crystals (white arrows) compared to the pristine plate-like crystal morphology (*) at the zone adjacent to cells. Scale bar:10 µm.
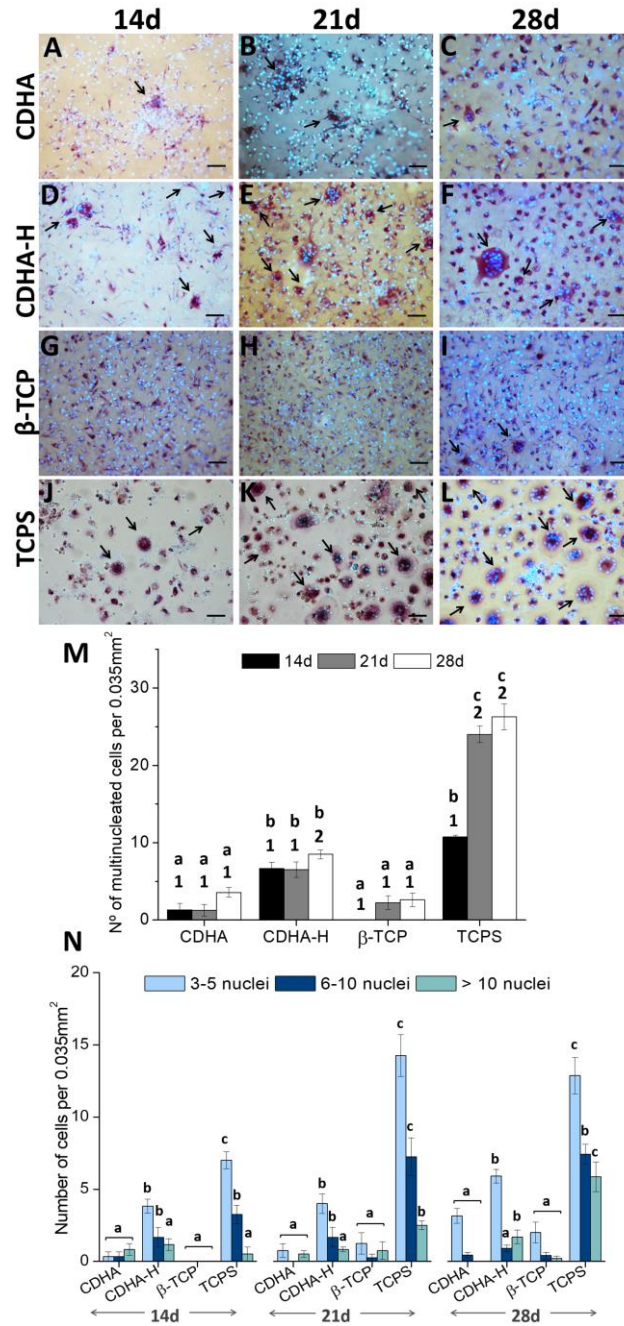
Figure 4. TRAP-Hoechst staining showing OCP differentiation over time on CDHA (A, B and C), CDHA-H (D, E and F), β-TCP (G, H and I) and TCPS (I, K and L).). Scale bar: 25 µm. Black arrows indicate multinucleated cells. M: Number of multinucleated cells on the different substrates at each time point analyzed by ImageJ. Groups identified by the same superscripts are not statistically different (p>0.05). Numbers indicate differences between time points for each substrates, and letters indicate differences between substrates at each time point. N: Distribution of multinucleated cells according to the number of nuclei at different time points of culture. Letters indicated differences in substrates for each type of multinucleated cells within the same time points.
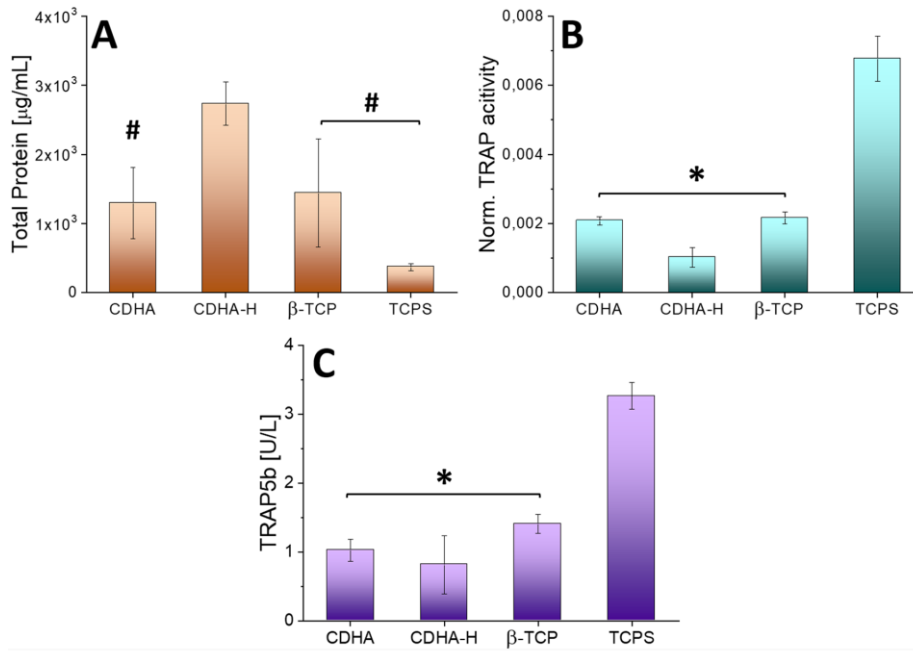
Figure 5. OC TRAP activity (A and B), and TRAP5b release (C). A: Total protein in the OCP cells cultured for 28 days, determined in the cell lysates by BCA (# indicates differences compared to CDHA-H); B: TRAP activity normalized to total protein in the cell lysates (* indicates differences compared to TCPS); C: TRAP5b isoform enzyme released in the supernatants, measured by ELISA (* indicates differences compared to TCPS). Statistical significance level established at $p < 0.05$.
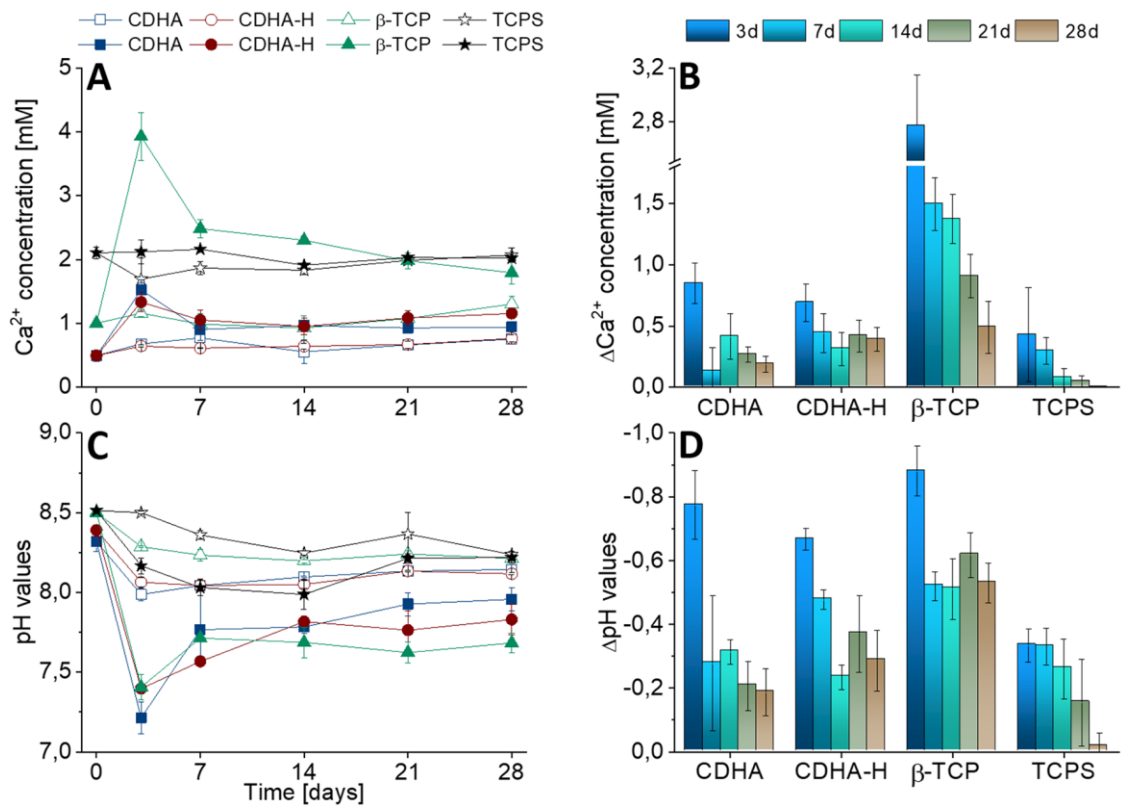
Figure 6. Evolution of the extracellular calcium concentration (A) and pH values (C) in the cell culture medium in presence (full symbols) and absence (hollow symbols) of OCP cells from 0 days (after preconditioning) to 28 days. Each time point represents the average of triplicates, with the corresponding standard deviation. The relative variation of calcium and pH with cells compared to that without cells are represented in B and D.

Graphical Abstract